

Chemical Potential, Helmholtz Free Energy and Entropy of Argon with Kinetic Monte Carlo Simulation

Chunyan Fan ^a, D. D. Do ^{a*}, D. Nicholson ^a and E. Ustinov ^b

^aSchool of Chemical Engineering, University of Queensland, St. Lucia, Qld 4072, Australia

^bIoffe Physical-Technical Institute of the Russian Academy of Sciences, 26 Polytechnicheskaya, St. Petersburg 194021, Russia

Abstract

We present a method, based on kinetic Monte Carlo (*kMC*), to determine the chemical potential, Helmholtz free energy and entropy of a fluid within the course of a simulation. The procedure requires no recourse to auxiliary methods to determine the chemical potential, such as the implementation of a Widom scheme in Metropolis Monte Carlo simulations, as it is determined within the course of the simulation. The equation for chemical potential is proved, for the first time in the literature, to have a direct connection with the inverse Widom potential theory in using the real molecules, rather than the ghost molecules. We illustrate this new procedure by several examples, including: fluid argon and adsorption of argon as a non-uniform fluid on a graphite surface and in slit pores.

* Author to whom all correspondence should be addressed. Email: d.d.do@uq.edu.au

1. Introduction

The Monte Carlo method, based on the Metropolis algorithm (*M-MC*) for importance sampling, has been widely applied to solve numerous equilibrium problems in physical chemistry and chemical engineering [1]. Recently we introduced a scheme based on kinetic Monte Carlo (*kMC*) as an alternative to *M-MC*, and have successfully applied it to describe vapour-liquid equilibria of fluids and adsorption on surfaces and in the confined spaces of pores [2-5]. The 2D-gas-solid, 2D-gas-liquid and order-disorder transitions of argon adsorption on a surface have also been successfully studied using this method [3]. Knowledge of thermodynamic variables such as chemical potential, entropy, Helmholtz and Gibbs free energy is essential to a complete understanding of the equilibrium state of a system. In *M-MC* in the canonical (*NVT*) or isothermal-isobaric (*NPT*) ensembles, the chemical potential is usually determined by the Widom method based on the potential distribution theory [6, 7]. The determination of the Helmholtz energy and entropy in *M-MC* however, has been a challenge in molecular simulation [1], and numerous methods have been proposed [8-11]. However, these are either theoretically complex or complicated to implement; readers are referred to Frenkel and Smit [1] for a review of this topic.

In this paper, we develop a simple but effective *kMC* method to calculate the chemical potential, the Helmholtz free energy and the entropy during the course of a simulation without the need for any additional procedures. We illustrate our scheme with simulations of fluid argon and argon adsorbed on a graphite surface and in slit pores. Other complex fluids and mixtures can be handled in the same way, and will be the subject of future investigations.

2. Theory

2.1 Kinetic Monte Carlo

Details of our *kMC* method have been given in previous publications [2-4], where we have presented an equation for the chemical potential. Before discussing the appropriate equations for the thermodynamic properties, we briefly review the *kMC* technique presented in earlier work.

2.1.1 Molecular energy

The basic variable in the *kMC* method, is the molecular interaction energy. In a canonical simulation the molecular energy of molecule *i* is the sum of pairwise interaction energies with all other molecules and with the surface, if present, and is given by:

$$u_i = \sum_{\substack{j=1 \\ j \neq i}}^N \varphi_{i,j} + \varphi_{i,s} \quad (1)$$

where $\varphi_{i,j}$ is the pairwise interaction energy between molecules i and j , and $\varphi_{i,s}$ is the interaction energy of molecule i with the solid surfaces. Here we use the symbols φ for the pairwise interactions to distinguish this interaction energy from u for the molecular energy. The upper case U will denote the configurational energy of the system.

2.1.2 Molecular mobility

The mobility of a molecule with energy u_i is calculated from:

$$\nu = \exp\left(\frac{u_i}{kT}\right) \quad (2)$$

therefore those molecules having larger values of u_i will have higher mobilities, and a greater tendency to move. For example, overlapping molecules having positive molecular energies will be more likely to move in order to break away from an overlapping configuration; on the other hand, molecules attracted to a solid surface or in the vicinity of other molecules at around the potential minimum separation, have negative molecular energies and will be less mobile. To highlight the large range of possible mobilities, we consider two examples for argon ($\sigma = 0.3405\text{nm}$ and $\varepsilon/k = 119.8\text{K}$) at 87.3K : (1) a pair of overlapping molecules with separation 0.785σ , for which $u_i/kT=100$ and $\exp(u_i/kT)=10^{43}$, and (2) a pair of argon atoms at the equilibrium separation of $2^{1/6}\sigma$, where $\exp(u_i/kT)=0.25$.

2.1.3 Duration of a given configuration

Since each molecule in the simulation box has its own mobility, the sum of mobilities for N molecules is a measure of the energetic state of a given configuration:

$$R_N = \sum_{i=1}^N \nu_i = \sum_{i=1}^N \exp\left(\frac{u_i}{kT}\right) \quad (3)$$

This is a measure of the speed at which the system would evolve from its current configuration; the duration of this configuration is therefore given by [12]:

$$\Delta t = \frac{1}{R_N} \ln\left(\frac{1}{p}\right) \quad (4)$$

where p is a random number ($0 < p < 1$), generated for this configuration, and ensures that configurations having the same total rate, R_N , are generated according to the Poisson law of distribution.

Equations (3 and 4) mean that the duration is a measure of how mutually attractive or repulsive the system is. The system is neutral when $u_i = 0$ for all i and hence the average duration is equal to $1/N$. If the duration is greater than $1/N$, the system provides an attractive environment, while a value smaller than $1/N$ means that the system is repulsive. This means is that the product of N and the average duration has a special significance as we shall show below when we discuss the chemical potential.

2.1.4 Generation of a Configuration

The *kMC* procedure involves only one move to generate a new configuration: the deletion of a randomly selected molecule from its current position and re-insertion of the molecule at a random position and orientation (i.e. uniform sampling) in the simulation box [2]. The *kMC* algorithm is therefore rejection-free. The selection of a molecule is based on the Rosenbluth criterion; the k -th molecule being selected according to:

$$R_{k-1} \leq pR_N < R_k \quad (5)$$

where p is a random number, R_N is the total mobility (eq.3) and R_k is the partial sum of the molecular mobilities from molecule 1 to molecule k :

$$R_k = \sum_{i=1}^k v_i \quad (6)$$

2.1.5 Overlapping molecules

Since molecular overlap can give very large positive values of energy, we replace the criterion in eq.(5) with its logarithm for the purpose of implementing the algorithm:

$$X_{k-1} \leq \ln p + X_N < X_k \quad (7)$$

where $X = \ln R$.

The criteria of eq.(5) or (7) imply that molecules having large energies have a greater chance of being selected, but the chosen molecule is not necessarily the one having the largest molecular energy and therefore the stochastic nature of the process is maintained.

To avoid infinitely large energies from molecular overlap, pairwise potential energies greater than a threshold value ϕ^* (which is a large positive number), are assigned ϕ^* as their pairwise potential energy. When the threshold value is reached, the duration of the configuration would be

so small its contribution to the time averaging process would be infinitesimally small; hence, the results are insensitive to the selection of this value. Further details can be found in ref [13].

2.1.6 Computational Considerations

Rosenbluth criterion

For the purpose of computation, the Rosenbluth selection can be made in a more efficient manner using a recurrence formula (Appendix 3). For example, for a given configuration, the array X_k ($k=1, 2, \dots, N$) can be calculated from:

$$X_k = X_{k-1} + \ln[1 + e^\Delta] \quad \text{if } \Delta < 0 \quad (8a)$$

$$X_k = (u_k / kT) + \ln[1 + e^{-\Delta}] \quad \text{if } \Delta > 0 \quad (8b)$$

where $\Delta = (u_k / kT) - X_{k-1}$. The starting value is $X_1 = u_1 / kT$. Once this array, of dimension N , has been calculated, the duration of the current configuration is given by

$$\Delta t = \exp(-X_N) \ln(1/p) \quad (9)$$

and the selection of the molecule to be moved in order to generate the next configuration is made with eq.(7).

When a selected molecule is moved to a new position, it is necessary to re-compute the molecular energies of all molecules. However, since the move only changes the pairwise interaction energies between the selected molecule and the rest, we only need to replace the “old” pairwise interaction energies with the “new” one (see Appendix 1 for details).

2.2 Output from the kMC simulation

2.2.1 Excess amount

When the system is an adsorption system, the excess amount (i.e. the amount that is associated with adsorption) is defined as:

$$N_{ex} = N - V\rho_G \quad (10)$$

where V is the volume accessible to the centre of mass of a molecule. The gas density is calculated in a region far away from the surface where the solid-fluid interactions are negligible. When the adsorbent is a confined space the external gas space is connected to the confined space, and the simulation box is a combination of these two spaces [4].

2.2.2 Chemical Potential

The chemical potential is determined by using molecules moved in the simulation to probe the volume space uniformly, allowing us to scan the energy space; this is equivalent to the inverse potential theory of Widom [6, 7]; further details are given in Appendix 2.

After M *kMC* simulation steps (usually of the order of 10 million) the chemical potential is obtained from the following equation (eq.A2.24 in Appendix 2)

$$\mu = kT \ln \left(\frac{\Lambda^3 \langle R_N \rangle}{V} \right) = kT \ln \left(\frac{\Lambda^3 N}{V} \right) + kT \ln \left(\frac{\langle R_N \rangle}{N} \right) \quad (11)$$

The first term on the *RHS* is the chemical potential of an ideal gas and the second term is the excess chemical potential. Here Λ is the thermal de Broglie wavelength, and $\langle R_N \rangle$ is the average total mobility, weighted by the duration of each configuration given by:

$$\langle R_N \rangle = \sum_{j=1}^M (R_N)_j \alpha_j; \quad \alpha_j = \frac{(\Delta t)_j}{\sum_{k=1}^M (\Delta t)_k} = \frac{(\Delta t)_j}{T_M} = \frac{1}{T_M} \frac{\ln(1/p_j)}{(R_N)_j} \quad (12a)$$

where, from eq. (4), α_j is the fraction of time for which the configuration j exists and T_M is the simulation time after M steps. Eq.(12a) can be simplified to give:

$$\langle R_N \rangle = \frac{M}{T_M} = \frac{1}{\bar{T}_M} \quad (12b)$$

since, $\sum_j \ln(1/p_j) = 1$ for a uniform distribution of random numbers. \bar{T}_M is the average duration of a configuration.

Thus the chemical potential in eq.(11) is:

$$\mu = kT \ln \left(\frac{\Lambda^3 N}{V} \right) + kT \ln \left(\frac{1}{N \bar{T}_M} \right) \quad (12c)$$

For ideal gases, it follows from eq.(3) that $\bar{T}_M = 1/N$ since $u_i=0$ and therefore the chemical potential in eq.(12c) reduces to the ideal gas expression.

Eq. (12c) corroborates our earlier remarks about the average duration of a configuration. When the system is neutral, i.e. there is no attraction or repulsion (as in the ideal gas), the product $N\bar{T}_M$ is equal to unity, and the excess chemical potential is zero. On the other hand, in an attractive environment, such as a stable liquid or a real gas, $N\bar{T}_M$ is greater than unity, and the excess

chemical potential is negative; conversely the excess chemical potential is positive in a repulsive environment.

2.2.3 Helmholtz free energy and entropy

In a canonical ensemble at equilibrium the Helmholtz free energy is a minimum and

$$\left(\frac{\partial F}{\partial N}\right)_{V,T} = \mu \quad (13)$$

Therefore, the Helmholtz free energy can be obtained by integration once $\mu(N)$ is known [5]:

$$F(N) - F(N_G) = \int_{N_G}^N \mu(N) dN \quad (14)$$

where $F(N_G)$ is the Helmholtz free energy of an ideal gas of N_G molecules and is given by

$$F(N_G) = N_G \mu(N_G) - N_G kT \quad (15)$$

The integral molecular Helmholtz free energy is $F(N)/N$.

The entropy of N molecules and the work done by the system can be calculated as

$$\langle F \rangle = E_K + \langle U \rangle - \langle S \rangle T \quad (16)$$

$$\langle P \rangle V = N\mu - \langle F \rangle \quad (17)$$

where E_K is the kinetic energy, $E_K = (3/2)NkT$ for a monatomic gases, $\langle U \rangle$ is the ensemble averaged configurational energy of N molecules and S is the entropy. Eq. 17 allows us to determine the pressure of the system by the thermodynamic route.

2.2.4 Virial pressure via the mechanical route and bulk gas density:

The pressure can be calculated via the virial route by combining *kMC* with the bin-concept of Fan *et al.* [14]. A bulk gas volume, either isolated or connected to the adsorption system, is set up. A molecule is selected according to the Rosenbluth algorithm from all the molecules in the adsorption volume and the gas volume; it is then placed at a random position in either the adsorption box or the gas box with a probability proportional to their respective volumes.

The pressure of the gas in the bulk gas box can be calculated from:

$$P = \rho_G k_B T - \frac{\bar{A}}{3V_1} \quad (18a)$$

where \bar{A} is the time average of the virial A , which is defined as follows:

$$A = \sum_{i=1}^{N_1-1} \sum_{\substack{j \in V_1 \\ j=i+1}}^{N_1} r_{i,j} \frac{d\varphi(r_{i,j})}{dr_{i,j}} + \frac{1}{2} \sum_{i \in V_1} \sum_{j \in V_1} r_{i,j} \frac{d\varphi(r_{i,j})}{dr_{i,j}} \quad (18b)$$

Here N_1 is the number of molecules in the bulk gas volume V_1 , and r_{ij} is the distance between the centres of molecules i and j . The density of the bulk gas can be calculated from:

$$\rho_G = \sum_{k=1}^M (N_{1,k} / V_1) \alpha_k \quad (18c)$$

where the subscript k denotes configuration and α_k is calculated from eq.(12a).

3. Results and Discussion

To illustrate the calculation of chemical potential, Helmholtz free energy, pressure and entropy using *kMC* we chose the following systems, with argon as a model molecule:

1. Uniform fluid
 - 1.1 At the sub-critical temperature 87K with densities covering the change from gas to liquid states passing through the unstable transition state.
 - 1.2 At the supercritical temperature 240K.
2. Argon adsorbed at 87K on a graphite surface
3. Argon adsorbed at 87K in slit pores of width 0.8nm and 1nm to study commensurate and incommensurate packings.

3.1 Uniform fluid at 87.3K and 240K

The simulation box was cubic with dimensions of $5\sigma \times 5\sigma \times 5\sigma$, and 10^7 *kMC* steps were used for both the equilibration and sampling stages. The energy limit u_k/kT was set at 100.

3.1.1 Average time per configuration

The variables that are of interest in the calculation of the chemical potential are the average duration time, \bar{T} , and the product $N\bar{T}$ (see eq.12c). They are shown in Figure 1 as a function of number of molecules. The average times at different temperatures approach the asymptote to $1/N$ (dashed line in Fig.1) as predicted by the ideal gas condition (eq.12c), when the number of molecules becomes very small. The average time at 240K reaches this asymptote at a higher density than at 87K, as would be expected at higher temperatures.

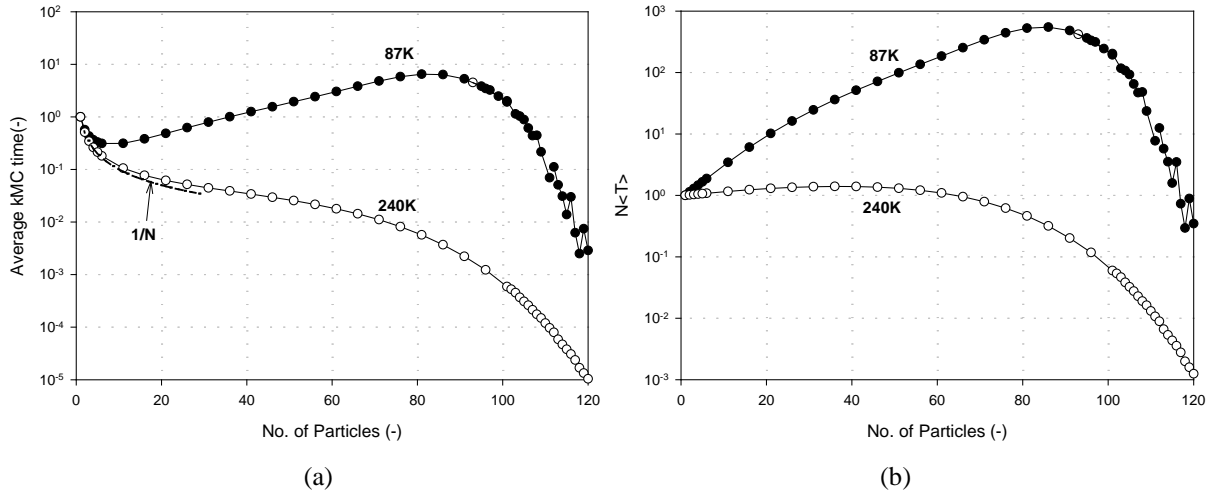


Figure 1: Plot of (a) the average time and (b) $N\bar{T}$ versus number of molecules for bulk argon at 87K and 240K. The density, $\rho^* = \rho\sigma^3$, is $N/(5 \times 5 \times 5)$.

The product $N\bar{T}$ (Fig.1b) for fluid argon is equal to unity in the ideal gas state at both temperatures, as required by the ideal gas condition. At 87K, it first increases above unity as N is increased; as expected when there is net attraction between molecules. $N\bar{T}$ reaches a maximum at $N=85$ which corresponds to a density, $\rho^* = \rho\sigma^3 = 0.68$ or a molar density of 28.6 kmol/m^3 . This density corresponds to the liquid spinodal point of LJ argon at 87K. For densities greater than this the product $N\bar{T}$ decreases, but remains above unity until the number of molecules exceeds 112 (corresponding to $\rho^* = \rho\sigma^3 = 0.9$, or $\rho = 37.7 \text{ kmol/m}^3$) when the system becomes repulsive.

At 240K, $N\bar{T}$ starts from unity in the ideal gas state, increases only modestly with N , and reaches a maximum at $N=40$, corresponding to $\rho^* = 0.32$, beyond which it decreases and falls below unity at $N=60$ or $\rho^* = 0.48$. This indicates that the system at 240K becomes repulsive at a rather moderate density because of the high kinetic energy that enables molecules to approach closer to each other and make frequent excursions into their repulsive cores. Above a reduced density of 0.48, the product $N\bar{T}$ decreases very steeply, because of the significant contribution from repulsion under supercritical conditions, even at moderate densities. The significance of repulsion under supercritical conditions has been discussed by Abdul Razak et al. [15].

3.1.2 Chemical Potential

Figure 2 shows the reduced chemical potential, μ/kT , at 87K and 240K versus N , the ideal gas and excess contributions, and the time-averaged configurational energies. At the sub-critical temperature of 87K, the ideal gas excess chemical potential is zero and the corresponding

reduced ideal gas chemical potential is -12.16. The excess chemical potential becomes negative (attractive) as N is increased and reaches a minimum at the liquid spinodal density, after which it increases and becomes zero at a reduced density of 0.9. Above this density, the excess chemical potential is positive; i.e. the system is repulsive as noted earlier for the product $N\bar{T}$ in Figure.1. The total chemical potential (the sum of the excess and ideal gas chemical potentials) is sigmoid (a van der Waals curve) as expected for sub-critical conditions.

At the supercritical temperature 240K, the total chemical potential increases continuously with density. When $N=60$ ($\rho^*=0.48$), the system switches from attractive to repulsive as evidenced by the positive excess chemical potential. The configurational energies decrease with density at both temperatures; the decrease being faster at 87K.

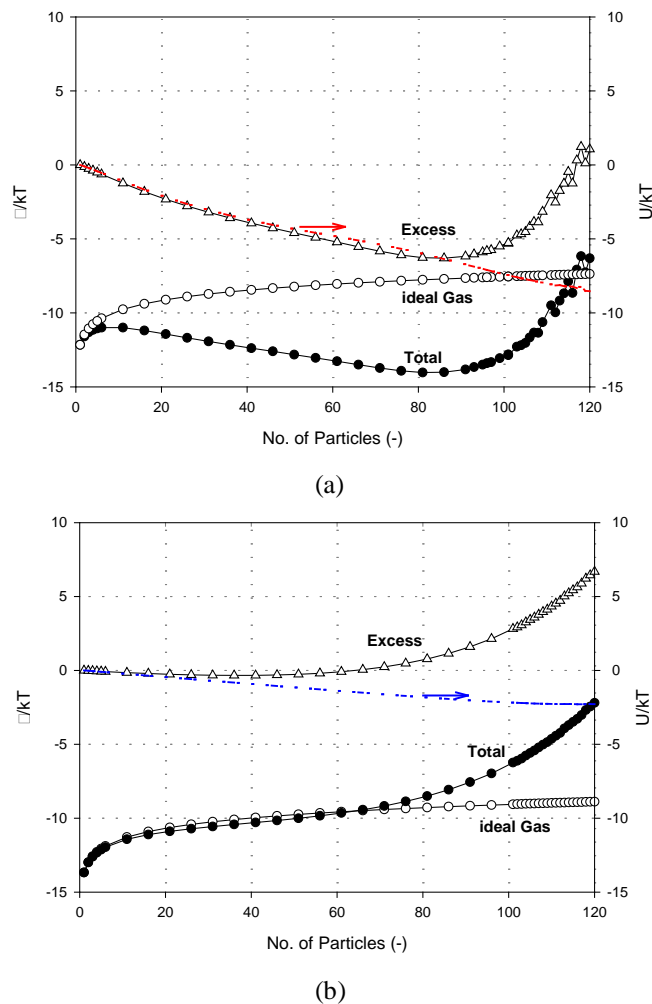


Figure 2: Plots of chemical potential and configuration energy versus number for fluid argon at (a) 87K and (b) 240K. The configuration energy is shown as a dashed line with the axis on the RHS of the graphs. The reduced density, $\rho^*=\rho\sigma^3$, is $N/(5\times 5\times 5)$.

The chemical potentials (kJ/mol) at 87K and 240K are shown in Figure 3 as a function of the number of molecules to illustrate their relative magnitudes. For a given density the chemical potential at 87K is always higher, implying that it is always higher at lower temperatures.

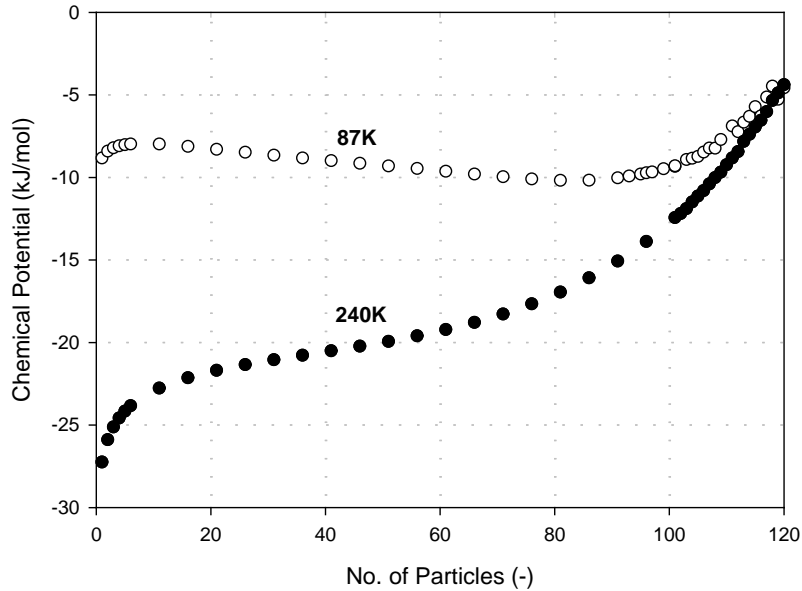


Figure 3: Chemical potential (kJ/mol) of LJ fluid argon at 87K and 240K obtained with *kMC*.

3.1.3 Molar Helmholtz Free Energy and Integral Molar Entropy

The Helmholtz free energy can be calculated from eq.14 using the plots of chemical potential versus density. Figure 4 shows the molar Helmholtz free energy and chemical potential of fluid argon at 87K and 240K; the results are in good agreement with the NIST data [16, 17]. At the supercritical temperature of 240K the chemical potential is always greater than the molar Helmholtz free energy. Since the difference between the Gibbs free energy and the Helmholtz free energy is the thermodynamic work, this means that the work is positive for all densities, and therefore work must be applied on the system to maintain it at equilibrium. At the subcritical temperature 87K there is an intermediate region where the molar Helmholtz free energy is greater than the chemical potential, and the thermodynamic work is therefore negative. It follows that the system has a tendency to evolve away from its current state, which is equivalent to saying that this region of intermediate densities is unstable at 87K (Figure 5). For densities less than or greater than these, the chemical potential is greater than the Helmholtz free energy; in these regions the system is in a stable (or metastable) gaseous or liquid state.

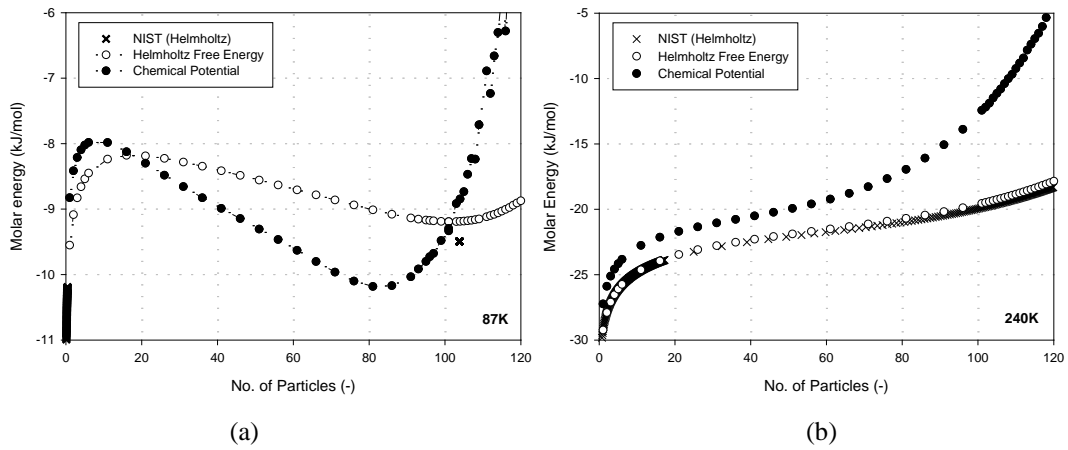


Figure 4: Integral molecular Helmholtz free energy and chemical potential as a function of number of particles for fluid argon at (a) 87K and (b) 240K

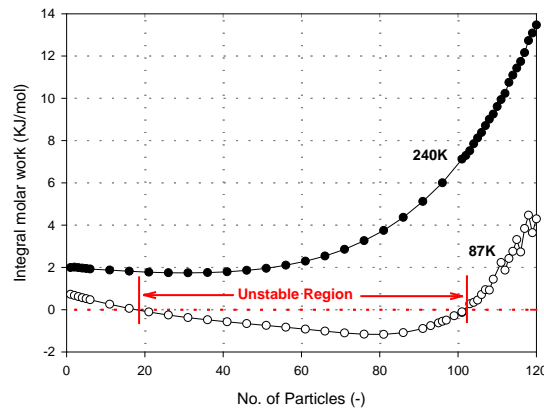


Figure 5: Integral molecular work as a function of number of particles for fluid argon at 87K and 240K

Figure 6 shows the integral molar entropy of fluid argon at 87K and 240K. At both temperatures the entropy decreases with density as the number of degrees of freedom decreases. At a given density, the molar entropy is higher at the higher temperature, because of its higher kinetic energy.

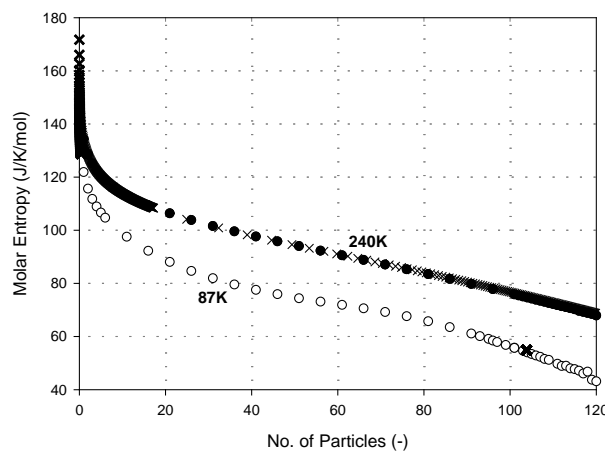


Figure 6: Integral molecular entropy as a function of number of particles for fluid argon at 87K and 240K

3.2 Argon Adsorption on Graphite at 87K

3.2.1 Average duration per configuration

The simulation box consisted of a 10σ square graphite base with a height of 100nm terminated by a hard wall. The height was large enough to ensure that the fluid in the top section of the box was essentially of uniform density, equivalent to that of the gas phase. 10^7 *kMC* steps were used for both the equilibration and sampling stages. As in the previous calculations, the energy limit for overlapping of molecules, u_k/kT , was set at 100. The average duration of a configuration and the product $N\bar{T}$ for argon adsorption on graphite at 87K are shown in Figure 7.

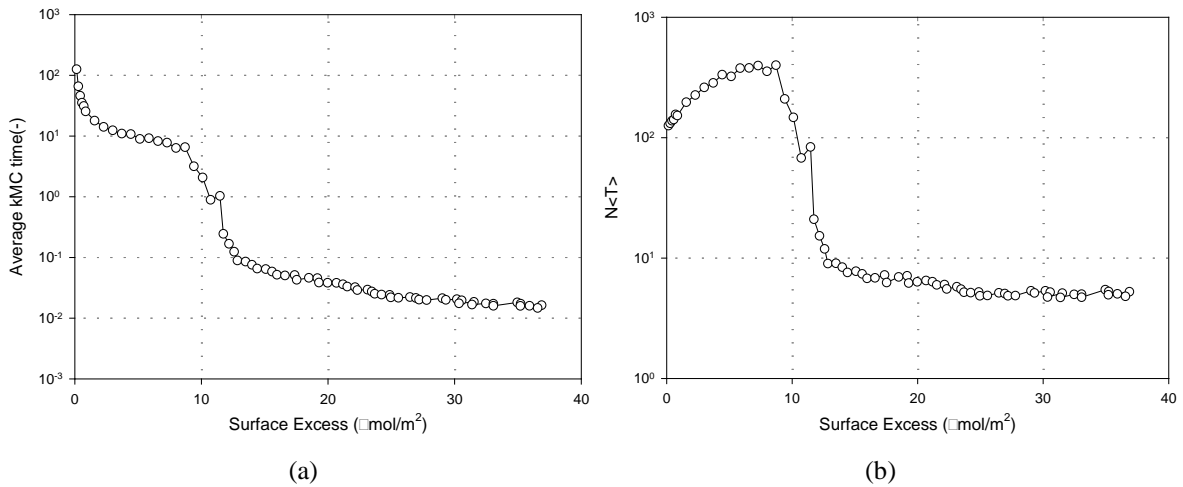


Figure 7: Plot of (a) the average time and (b) $N\bar{T}$ versus surface excess concentration for argon adsorption on graphite at 87K.

Unlike the fluid of uniform density, where the average time, \bar{T} , is unity at zero density, the average duration for argon adsorbed on graphite at 87.3K is 126 ± 1 , because of the strong attraction of the surface. This average time could be interpreted as a residence time for a molecule on the surface and would be expected to increase with the affinity between the adsorbate and the surface. The product $N\bar{T}$ rises to a maximum as the first layer is completed and then decreases, but always remains above unity, indicating that the adsorbate is in an attractive environment.

3.2.2 Chemical Potential and Molar Helmholtz Free Energy

Figure 8 shows plots of the chemical potential and the molar Helmholtz free energy versus surface excess density for argon adsorption at 87K.

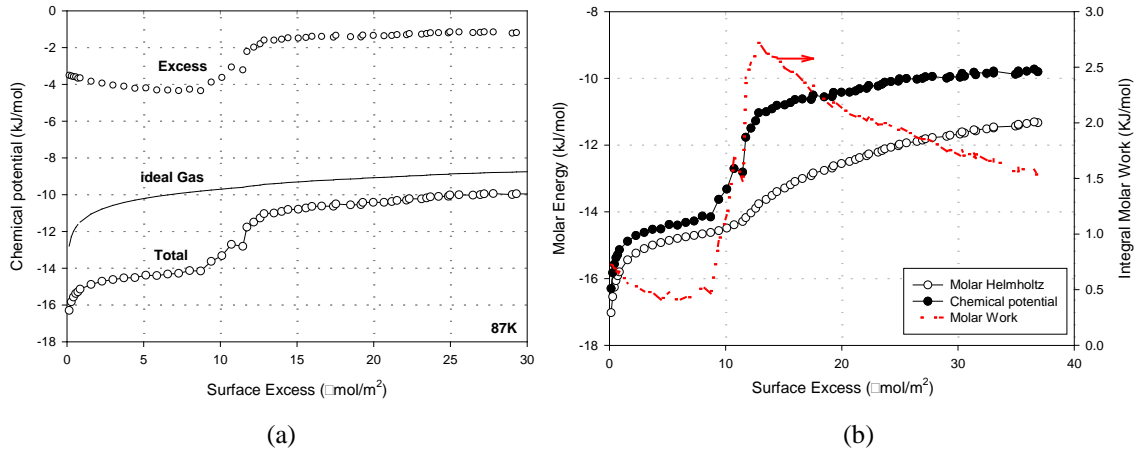


Figure 8: (a) Chemical potential versus the surface excess density and the contributions from excess and ideal gas; (b) plots of chemical potential and molar Helmholtz free energy versus surface excess density for argon adsorption on graphite at 87K; the molar work done by the system is shown in (b) as a dashed line and the axis is on the RHS.

Again in contrast to the fluid of uniform density (Section 3.1) the excess chemical potential is negative not zero at low density because of the attraction between a molecule and the surface.

As the surface loading is increased below the monolayer coverage (about $11\mu\text{mol/m}^2$), the excess chemical potential decreases due to the combination of the relatively constant solid-fluid interaction and increasing fluid-fluid interaction. As density is increased beyond monolayer coverage, the excess chemical potential, μ^{ex} , increases because of the reduction in the solid-fluid interaction for molecules further away from the surface, but remains negative because the system is overall attractive. The chemical potential is greater than the molar Helmholtz free energy, indicating that the systems are stable. The molar work (eq.(17), shown in Figure 8b, decreases with loading to a minimum in the sub-monolayer region, increases sharply to a maximum, and then decreases again as higher layers are formed.

The plot of molar entropy versus loading at 87K is given in Figure 9. In the sub-monolayer region (surface densities less than $11\mu\text{mol/m}^2$), the entropy decreases as the number of available configurations for monolayer molecules decreases, then increases again as molecules adsorb beyond a monolayer distance from the surface, and finally approaches the molar entropy of liquid-like argon as higher layers are built up. This confirms an earlier conclusion [18] that adsorbed argon approaches the liquid state as adsorption increases, and shows that this state is reached in this system when approximately two statistical monolayers have been adsorbed.

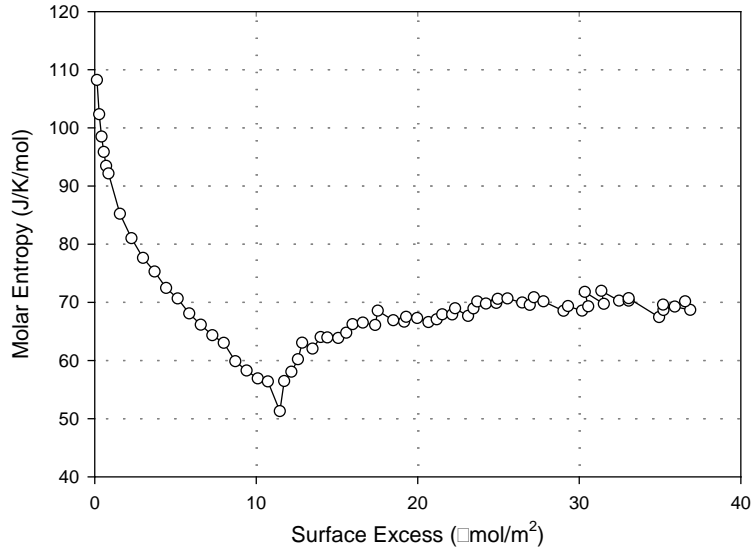


Figure 9: Integral molecular entropy versus surface excess density for argon adsorption on graphite at 87K.

3.3 Argon Adsorption in Slit Pores at 87K

The simulation box for studying the adsorption of argon in slit pores is shown in Figure 10: the slit pore (volume V_{II}) is connected to gas reservoirs with volumes V_I and V_{III} at the two ends of the pore.

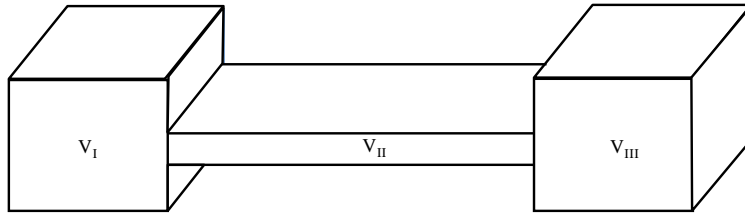


Figure 10: The schematic of the simulation box of adsorption in pores with kMC.

We considered two pore widths: 0.8nm and 1.0nm, the lengths of the pore in the other directions are both 5nm. The two gas reservoirs have dimensions: 5.0nm×10.0nm×10.0nm. 10^7 kMC steps were used in the equilibration and sampling stages.

The adsorption isotherms at 87K for 0.8nm and 1.0nm pores are presented in Figure 11. In the 0.8nm pore, adsorption follows a filling mechanism, typical of ultra fine micropores, while the isotherm for 1.0nm pore, is sigmoid, which is typical of a first order transition in the canonical ensemble [19]. The position of the equilibrium transition can be obtained from the Maxwell equal area construction applied to the plot of chemical potential versus number of molecules.

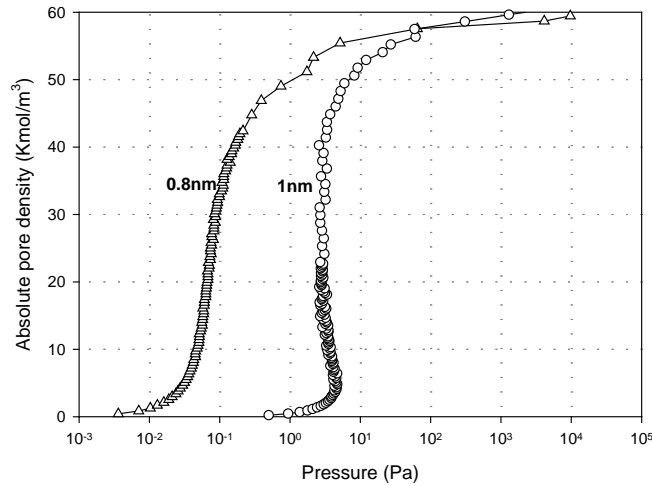


Figure 11: Plots of absolute pore density versus pressure for argon adsorption in slit pores with pore widths of 0.8nm and 1.0nm at 87K.

Figure 12 shows the average duration of a configuration and the product $N\bar{T}$ as a function of absolute pore density. There is a significant increase in average time in the smaller pore, compared to the 1.0nm pore, because of the deeper solid-fluid potential. At very high loadings, the average time is greater in the 1.0nm pore because this pore can pack two commensurate layers of adsorbate and there are therefore more adsorbate-adsorbate contacts.

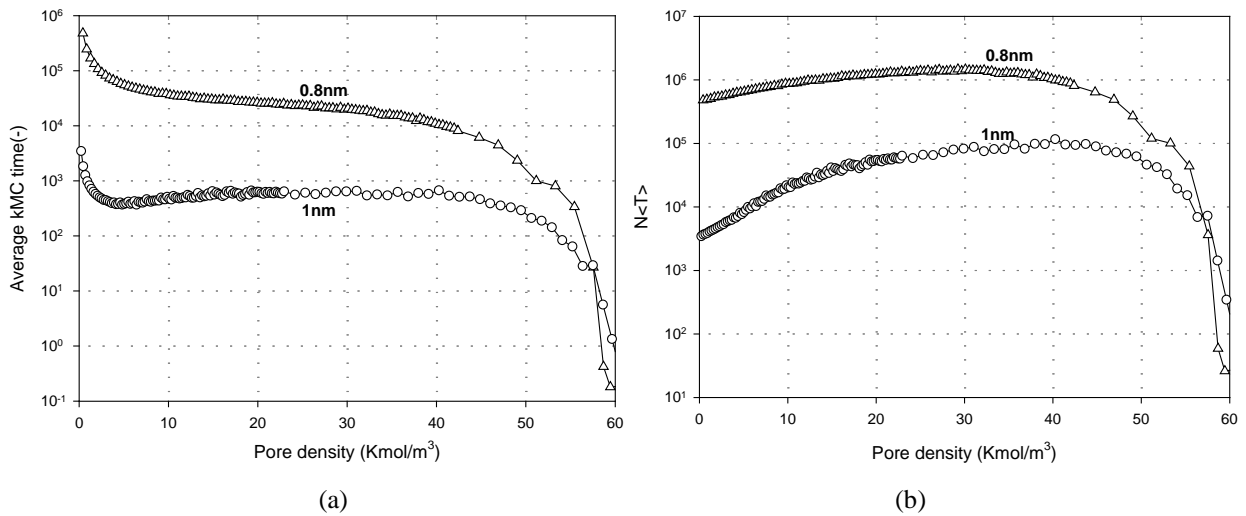


Figure 12: Plot of (a) the average time and (b) $N\bar{T}$ versus absolute pore density for argon adsorption in slit pores at 87K.

The plots of chemical potential and molar Helmholtz free energy versus pore density are shown in Figure 13. The lower chemical potential in the 0.8nm pore over most of the density range, and the cross over at high loading can again be attributed to the stronger solid-fluid potential in the 0.8nm pore and the increased number of adsorbate contacts in the 1.0nm pore at very high loading. Like the mean residence time in Fig.12, The chemical potential for the 1.0nm pore has a

(horizontal) sigmoid shape, which is typical of a system undergoing a first order transition. The work term calculated from eq. (17), shown in Figure 13c, is negative implying that the system is unstable as also noted for fluid argon at 87K.

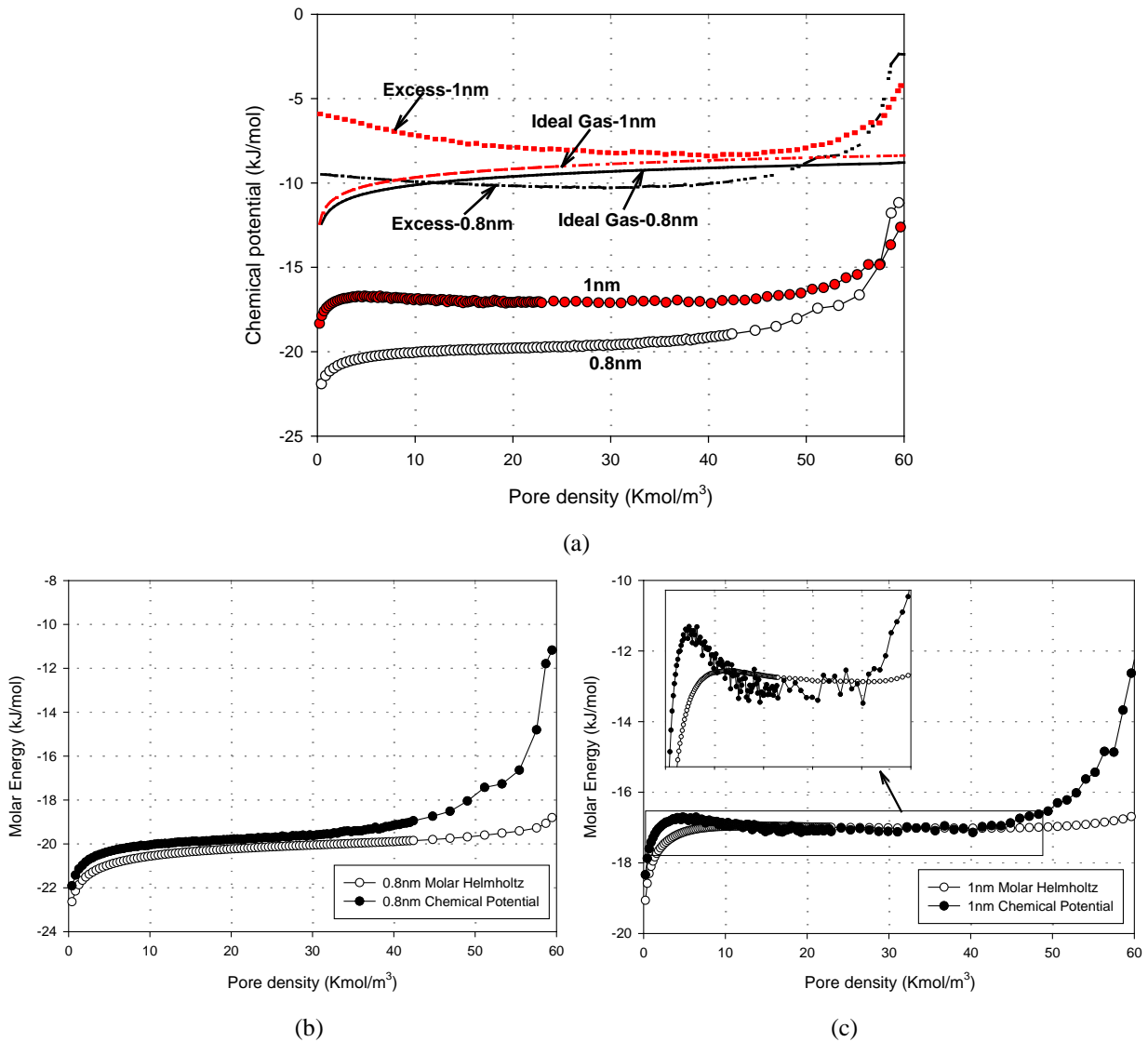


Figure 13: (a) Chemical potential versus the pore density and the contribution from excess and ideal gas; (b) and (c) plots of chemical potential and molar Helmholtz free energy versus pore density for argon adsorption in 0.8nm and 1.0nm pores at 87K, respectively.

Figure 14 shows the integral molar entropy versus pore density which decreases with density because of the loss of degrees of freedom. Interestingly, for a given density, the molar entropy in the 1.0nm pore is lower than in the 0.8nm pore because the packing is more efficient in the commensurate 1.0nm pore which can accommodate exactly two layers of argon; the 0.8nm pore is too large to accommodate one layer but too small to accommodate two layers, and therefore the packing is less efficient, resulting in a higher molar entropy.

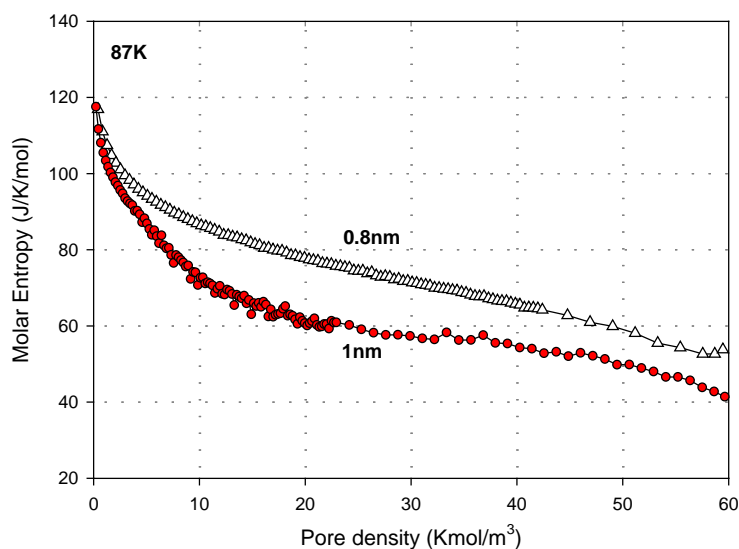


Figure 14: Integral molecular entropy versus pore density for argon adsorption in slit pores at 87K

4. Conclusions

The kinetic Monte Carlo method has been used to study bulk fluid argon, and argon adsorbed on a graphite surface and in slit pores, at both sub- and super-critical temperatures.

The method offers a distinct advantage over the conventional Metropolis scheme, in that chemical potential can be accurately and easily calculated at any density, in contrast to insertion methods that encounter well-known problems in high density regions.

Once chemical potential is known, it is straightforward to calculate other thermodynamic properties including, free energies and entropies. Implementation of the computational procedures is relatively simple compared to other approaches for obtaining these properties from simulation, and comparison with available data confirms that accurate results can be readily obtained.

Application of the kMC method to bulk fluid argon and argon adsorption at various temperatures gives a number of interesting features. The average kMC time for each configuration at zero loading increased with the strength of the adsorbent, suggesting a longer residence time of molecule spending on the surface. The product of the number of molecule and the average kMC time is a measure of the status of the system; it is attractive if this product is greater than unity while it is repulsive if it is less than unity. As a corollary, the excess chemical potential is

negative or positive for attractive or repulsive environment, respectively. The molar work of the system defined as the difference between the Gibbs and Helmholtz free energies is negative for unstable system, such as the unstable bulk fluid argon at 87K or the unstable region in pores whose canonical isotherms show a sigmoidal shape. The molar entropy is a measure of the degree of freedom. It continually decreases with density for uniform fluids, and for confined space it is lower for pores whose packing is commensurate; for example the molar entropy in 1nm pore is lower than that in 0.8nm pore because of the former can pack two integral layers of argon molecules.

Acknowledgement: This project is supported by the Australian Research Council. The author E. Ustinov acknowledges the support from the Russian Foundation for Basic Research.

Appendix 1: Updating of Molecular Energy when a Molecule is moved

After a molecule k has been moved to a new random position, the molecular interaction energies of all molecules are recalculated using eq. (1). Since the move only involves the molecule k , the molecular interaction energies can be updated as follows:

$$u_k^{new} = \sum_{\substack{i=1 \\ i \neq k}}^N \varphi_{k,i}^{new} \quad (\text{A1.1a})$$

$$u_i^{new} = u_i^{old} + (\varphi_{i,k}^{new} - \varphi_{i,k}^{old}); \text{ for } i \neq k \quad (\text{A1.1b})$$

Appendix 2: Chemical potential with potential distribution theory

Molecular simulation of equilibrium systems requires the determination of chemical potential to ensure that true equilibrium is established, especially in systems involving more than one phase or in systems that have a non-uniform distribution of density, where care must be taken to ensure that the chemical potential is the same everywhere inside the system.

In a Monte Carlo (*MC*) simulation with the Metropolis algorithm, the chemical potential is commonly calculated using the Widom method of test particle insertion or by the inverse Widom method of deleting a real particle from the simulation box (Widom, 1963, 1982). The forward method is suitable for systems whose configurations are determined with the Metropolis algorithm because the energy of interaction between a test particle (being inserted in a random position inside the box) and real particles, sample the full range of interaction energy, while the inverse method fails because the position of the deleted particle is favoured energetically by the Metropolis algorithm and therefore its energy of interaction with the remaining real particles does not sample the complete range of energy. However, the inverse Widom method is suitable for implementation in the *kMC* simulation because no position is favoured *a priori*. For the sake of completeness, we briefly describe both the forward and inverse Widom methods below.

Widom Forward method

In the classical limit, the partition function Q_{N+1} for a fluid of $N+1$ particles in a canonical ensemble is given by (Widom, 1963, 1982; Frenkel and Smit, 1996)

$$Q_{N+1} = \frac{1}{\Lambda^{3(N+1)} (N+1)!} \underbrace{\int_V \int_V \cdots \int_V}_{N+1 \text{ times}} \exp \left[-\frac{U_{N+1}(\underline{r}_1, \underline{r}_2, \cdots, \underline{r}_N, \underline{r}_{N+1})}{kT} \right] d\underline{r}_1 d\underline{r}_2 \cdots d\underline{r}_N d\underline{r}_{N+1} \quad (\text{A2.1})$$

which is the multiple volume integral of the Boltzmann factor of $N+1$ particles and $d\underline{r}_k$ is the volume element occupied by the k^{th} particle. The energy of interaction of $N+1$ particles can be calculated as the sum of all pairwise interaction energies, $\varphi_{i,j}$, and their interaction energies with the solid surfaces, $\varphi_{i,S}$:

$$U_{N+1}(\underline{r}_1, \underline{r}_2, \cdots, \underline{r}_N, \underline{r}_{N+1}) = \sum_{i=1}^N \sum_{j>i}^{N+1} \varphi_{i,j} + \sum_{i=1}^{N+1} \varphi_{i,S} \quad (\text{A2.2})$$

Let $(N+1)$ be a particle in the population, we can write the above interaction energy as the sum of the interaction energy of this particle with all the others plus the energy of interaction of the remaining N particles as follows:

$$U_{N+1}(\underline{r}_1, \underline{r}_2, \dots, \underline{r}_N, \underline{r}_{N+1}) = U_N(\underline{r}_1, \underline{r}_2, \dots, \underline{r}_N) + u_{N+1}(\underline{r}_1, \underline{r}_2, \dots, \underline{r}_N, \underline{r}_{N+1}) \quad (\text{A2.3})$$

where U_N is the energy of interaction among N particles, in which the $(N+1)^{\text{th}}$ particle is omitted:

$$U_N(\underline{r}_1, \underline{r}_2, \dots, \underline{r}_N) = \sum_{i=1}^{N-1} \sum_{j>i}^N \varphi_{i,j} + \sum_{i=1}^N \varphi_{i,S} \quad (\text{A2.4})$$

and

$$u_{N+1}(\underline{r}_1, \underline{r}_2, \dots, \underline{r}_N, \underline{r}_{N+1}) = \sum_{i=1}^N \varphi_{N+1,i} + \varphi_{N+1,S} \quad (\text{A2.5})$$

The partition function of a population of N particles, Q_N is given by

$$Q_N = \frac{1}{\Lambda^{3N} (N)!} \underbrace{\int_V \int_V \dots \int_V}_{N \text{ times}} \exp \left[-\frac{U_N(\underline{r}_1, \underline{r}_2, \dots, \underline{r}_N)}{kT} \right] d\underline{r}_1 d\underline{r}_2 \dots d\underline{r}_N \quad (\text{A2.6})$$

We would like to express the partition function of $N+1$ particles (eq. A1) and that of N particle (eq. A2.6). First we rewrite the partition function Q_{N+1} of eq. (A1) by making use of eq. (A2.3) as follows:

$$Q_{N+1} = \frac{1}{\Lambda^{3(N+1)} (N+1)!} \left\{ \underbrace{\int_V \int_V \dots \int_V}_{N \text{ times}} \Psi \exp \left[-\frac{U_N(\underline{r}_1, \underline{r}_2, \dots, \underline{r}_{N-1}, \underline{r}_N)}{kT} \right] d\underline{r}_1 d\underline{r}_2 \dots d\underline{r}_{N-1} d\underline{r}_N \right\} \quad (\text{A2.7a})$$

where

$$\Psi = \int_V \exp \left[-\frac{u_{N+1}(\underline{r}_1, \underline{r}_2, \dots, \underline{r}_N, \underline{r}_{N+1})}{kT} \right] d\underline{r}_{N+1} \quad (\text{A2.7b})$$

The multiple integral in eq. (A2.7a) can be integrated by Monte Carlo integration with N particles distributed in space according to the Metropolis scheme. This integral is:

$$\langle \Psi \rangle \underbrace{\int_V \int_V \dots \int_V}_{N \text{ times}} \exp \left[-\frac{U_N(\underline{r}_1, \underline{r}_2, \dots, \underline{r}_{N-1}, \underline{r}_N)}{kT} \right] d\underline{r}_1 d\underline{r}_2 \dots d\underline{r}_{N-1} d\underline{r}_N \quad (\text{A2.8a})$$

Combining this equation and eq. (A2.6), we get:

$$\langle \Psi \rangle Q_N \Lambda^{3N} N! \quad (\text{A2.8b})$$

where $\langle \Psi \rangle$ is the average based on N real particles, and it is calculated from eq. (A2.7b):

$$\langle \Psi \rangle = V \left\langle \exp \left[-\frac{u_{N+1}(\underline{r}_1, \underline{r}_2, \dots, \underline{r}_N, \underline{r}_{N+1})}{kT} \right] \right\rangle_N \quad (\text{A2.9})$$

The subscript N on the ensemble average means that the average is carried out with N particles frozen in space.

Combining eqs. (A2.7-9), we get:

$$Q_{N+1} = \frac{V}{\Lambda^3(N+1)} Q_N \left\langle \exp \left(-\frac{u_{N+1}}{kT} \right) \right\rangle_N \quad (\text{A2.10})$$

This canonical average can be computed by freezing N particles in space, and sampling the volume space by inserting the $(N+1)^{th}$ particle at a random position and determining the average according to the following equation:

$$\left\langle \exp \left(-\frac{u_{N+1}}{kT} \right) \right\rangle_V = \frac{1}{M} \sum_{j=1}^M \exp \left(-\frac{u_{N+1}}{kT} \right) \quad (\text{A2.11})$$

where M is the number of insertions of the test particle, u_{N+1} is the energy of interaction of the test particle at the random position j with the frozen N particles in space (calculated from eq. A2.5).

If we defined the activity Z as follows:

$$Z = \frac{Q_N}{\Lambda^3 Q_{N+1}} = \frac{(N+1)/V}{\left\langle \exp(-u_{N+1}/kT) \right\rangle_N} \quad (\text{A2.12})$$

this activity, in the limit of dilute system ($N \rightarrow 0$), will become the density because the interaction energy of the $(N+1)^{th}$ particle with the surrounding particles is zero. The ratio of the two partition functions is equal to $\exp(\mu/kT)$ [1], and therefore the activity is related to the chemical potential as follows:

$$Z = \frac{1}{\Lambda^3} \exp \left(\frac{\mu}{kT} \right) \quad (\text{A2.13})$$

This allows us to write the chemical potential as:

$$\mu = kT \ln \left[\Lambda^3 (N+1) / V \right] - kT \ln \left[\left\langle \exp \left(-\frac{u_{N+1}}{kT} \right) \right\rangle_N \right] \quad (\text{A2.14})$$

The first term on the *RHS* is the ideal gas chemical potential and the second term is the excess chemical potential. For the purpose of computation, the ensemble average in the second term of the above equation can be carried out as follows:

$$\left\langle \exp\left(-\frac{u_{N+1}}{kT}\right) \right\rangle_N = \frac{1}{N_t N_c} \sum_{j=1}^{N_c} \sum_{i=1}^{N_t} \exp\left(-\frac{u_{i,j}}{kT}\right) \quad (\text{A2.15})$$

where N_t is the number of test particles inserted for each configuration of N particles and N_c is the number of configurations that N -particles are frozen for the test insertion.

For polyatomic molecules, the test particle is given a random orientation for each insertion. To calculate the chemical potential in a given region of the system, the chemical potential for that region can be calculated from eq. (A2.14) and the variables in this equation are replaced by corresponding variables for the local region.

Real particle method of kMC :

From the partition function for $N-1$ particles, as given in eq. (A2.6) with N replaced by $N-1$, the interaction energy U_{N-1} replaced in terms of U_N and u_N , we have:

$$Q_{N-1} = \frac{1}{\Lambda^{3(N-1)} (N-1)!} \underbrace{\int_V \cdots \int_V}_{N-1 \text{ times}} \exp\left[-\frac{U_N(\underline{r}_1, \underline{r}_2, \dots, \underline{r}_{N-1}, \underline{r}_N)}{kT} + \frac{u_N(\underline{r}_1, \underline{r}_2, \dots, \underline{r}_{N-1}, \underline{r}_N)}{kT}\right] d\underline{r}_1 d\underline{r}_2 \cdots d\underline{r}_{N-1} \quad (\text{A2.16})$$

where N is an arbitrary particle. Multiplying this equation by

$$1 = \frac{1}{V} \int_V d\underline{r}_N \quad (\text{A2.17})$$

we get:

$$Q_{N-1} = \frac{1}{\Lambda^{3(N-1)} (N-1)! V} \underbrace{\int_V \cdots \int_V}_{N \text{ times}} \exp\left[-\frac{U_N(\underline{r}_1, \underline{r}_2, \dots, \underline{r}_{N-1}, \underline{r}_N)}{kT} + \frac{u_N(\underline{r}_1, \underline{r}_2, \dots, \underline{r}_{N-1}, \underline{r}_N)}{kT}\right] d\underline{r}_1 d\underline{r}_2 \cdots d\underline{r}_{N-1} d\underline{r}_N \quad (\text{A2.18a})$$

or

$$Q_{N-1} = \frac{1}{\Lambda^{3(N-1)} (N-1)! V} \underbrace{\int_V \cdots \int_V}_{N \text{ times}} \Omega \exp\left[-\frac{U_N(\underline{r}_1, \underline{r}_2, \dots, \underline{r}_{N-1}, \underline{r}_N)}{kT}\right] d\underline{r}_1 d\underline{r}_2 \cdots d\underline{r}_{N-1} d\underline{r}_N \quad (\text{A2.18b})$$

where

$$\Omega = \exp\left[\frac{u_N(\underline{r}_1, \underline{r}_2, \dots, \underline{r}_{N-1}, \underline{r}_N)}{kT}\right] \quad (\text{A2.19})$$

The multiple integral of eq. (A2.18) can be determined by Monte Carlo integration giving:

$$\langle\langle\Omega\rangle\rangle = \frac{\int \cdots \int_{\substack{V \\ N \text{ times}}} \Omega \exp\left[-\frac{U_N(\underline{r}_1, \underline{r}_2, \dots, \underline{r}_{N-1}, \underline{r}_N)}{kT}\right] d\underline{r}_1 d\underline{r}_2 \cdots d\underline{r}_{N-1} d\underline{r}_N}{\int \cdots \int_{\substack{V \\ N \text{ times}}} \exp\left[-\frac{U_N(\underline{r}_1, \underline{r}_2, \dots, \underline{r}_{N-1}, \underline{r}_N)}{kT}\right] d\underline{r}_1 d\underline{r}_2 \cdots d\underline{r}_{N-1} d\underline{r}_N} \quad (\text{A2.20})$$

The ensemble average is determined with N real particles. Combining this with the partition for N particles (eq. A2.6), we get:

$$Q_{N-1} = \frac{\Lambda^3 N}{V} Q_N \left\langle\left\langle \exp\left[\frac{u_N(\underline{r}_1, \underline{r}_2, \dots, \underline{r}_{N-1}, \underline{r}_N)}{kT}\right] \right\rangle\right\rangle \quad (\text{A2.21})$$

The canonical average is for the N -particle system, and is suitable for the determination of the chemical potential in the kMC scheme.

Thus, the activity is:

$$Z = \frac{1}{\Lambda^3} \frac{Q_{N-1}}{Q_N} = \frac{1}{\Lambda^3} \exp\left(\frac{\mu}{kT}\right) = \frac{N}{V} \left\langle\left\langle \exp\left[\frac{u_N(\underline{r}_1, \underline{r}_2, \dots, \underline{r}_{N-1}, \underline{r}_N)}{kT}\right] \right\rangle\right\rangle \quad (\text{A2.22})$$

and this allows us to derive an equation for the chemical potential in the kMC scheme:

$$\mu = kT \ln(\Lambda^3 \rho) + kT \ln\left(\left\langle\left\langle \exp\left(\frac{u_k}{kT}\right) \right\rangle\right\rangle\right) \quad (\text{A2.23a})$$

where u_k is the interaction energy of the real k -particle in the N -particle system, and $\langle\langle \rangle\rangle$ is the canonical average of the real particle in the N -particle system. In the kMC scheme, this average is calculated as follows:

$$\left\langle\left\langle \exp\left(\frac{u_k}{kT}\right) \right\rangle\right\rangle = \frac{\sum_j \left[\frac{1}{N} \sum_{k=1}^N \exp\left(\frac{u_{k,j}}{kT}\right) \right] \Delta t_j}{\sum_j \Delta t_j} = \frac{1}{N} \langle R_N \rangle \quad (\text{A2.23b})$$

where Δt_j is the duration of the configuration j . Combining eqs. (A2.23a) and (A2.23b), we get the required equation for the chemical potential:

$$\mu = kT \ln\left(\frac{\Lambda^3}{V} \langle R_N \rangle\right) \quad (\text{A2.24})$$

Using real particles in calculating the chemical potential in the kMC scheme affords a great advantage over the traditional test particle method because (1) the energy of interaction of real

particle samples the whole energy space since the kMC , allows for overlap between molecules and (2) the enormous value of $\exp(u/kT)$ is compensated by the very small duration, Δt , of that specific configuration.

In systems with non-uniform density, such as adsorption systems or two-phase systems, we can calculate the chemical energies in various regions of the system. Then the chemical potential for a particular region, say region Ω , is calculated from:

$$\left\langle\left\langle \exp\left(\frac{u_k}{kT}\right) \right\rangle\right\rangle_{\Omega} = \frac{\sum_j \left[\frac{1}{N_{\Omega}} \sum_{k \in \Omega} \exp\left(\frac{u_{k,j}}{kT}\right) \right] \Delta t_j}{\sum_j \Delta t_j} \quad (\text{A2.25})$$

where N_{Ω} is the number of particles in that region and u_k is the energy of interaction of the particle k in the same region.

Appendix 3: Recurrence formula for X

To obtain the total mobility, we consider its logarithm:

$$X_N = \ln R_N \quad (\text{A3.1})$$

Combining this equation and eq. (3), we get:

$$e^{X_N} = \sum_{i=1}^N \exp\left(\frac{u_i}{kT}\right) \quad (\text{A3.2})$$

By splitting the last term from the *RHS* of the above equation, we have:

$$e^{X_N} = \left(\sum_{i=1}^{N-1} e^{u_i/kT} \right) + e^{u_N/kT} = e^{X_{N-1}} + e^{u_N/kT} \quad (\text{A3.3a})$$

or generally

$$e^{X_k} = e^{X_{k-1}} + e^{u_k/kT} \quad (\text{A3.3b})$$

This is a recurrence formula for X_k ($k = 1, 2, \dots, N$), with the starting value $X_1 = u_1 / kT$. The recurrence formula of eq. (A3.3) can be computed as follows, depending on the sign of

$\Delta = (u_k / kT) - X_{k-1}$:

$$X_k = X_{k-1} + \ln \left[1 + e^{(u_k/kT) - X_{k-1}} \right] \quad \text{if } \Delta < 0 \quad (\text{A3.4a})$$

$$X_k = (u_k / kT) + \ln \left[1 + e^{X_{k-1} - (u_k/kT)} \right] \quad \text{if } \Delta > 0 \quad (\text{A3.4b})$$

References

1. D. Frenkel and B. Smit, *Understanding molecular simulation : From algorithms to applications*. Second ed. Computational Science Series, ed. D. Frenkel, et al. 2002, San Diego: Academic Press. 638.
2. E.A. Ustinov and D.D. Do, *Application of kinetic Monte Carlo method to equilibrium systems: Vapour–liquid equilibria*. Journal of Colloid and Interface Science, 2012. **366**(1): p. 216-223.
3. E.A. Ustinov and D.D. Do, *Two-dimensional order-disorder transition of argon monolayer adsorbed on graphitized carbon black: Kinetic Monte Carlo method*. J. Chem. Phys., 2012. **136**: p. 134702/1-134702/10.
4. V.T. Nguyen, D.D. Do, D. Nicholson, and E.A. Ustinov, *Application of the kinetic Monte Carlo method in the microscopic description of argon adsorption on graphite*. Mol. Phys., 2012: p. Ahead of Print.
5. E.A. Ustinov and D.D. Do, *Thermodynamic Analysis of Ordered and Disordered Monolayer of Argon Adsorption on Graphite*. Langmuir, 2012. **28**(25): p. 9543-9553.
6. Widom, *Some topics in the theory of fluids*. Journal of Chemical Physics, 1963. **39**(11): p. 2808-2812.
7. B. Widom, *Potential-distribution theory and the statistical mechanics of fluids*. The Journal of Physical Chemistry, 1982. **86**(6): p. 869-872.
8. J. Puibasset, *Grand Potential, Helmholtz Free Energy, and Entropy Calculation in Heterogeneous Cylindrical Pores by the Grand Canonical Monte Carlo Simulation Method*. The Journal of Physical Chemistry B, 2005. **109**(1): p. 480-487.
9. S. Prestipino and P. Giaquinta, *Statistical Entropy of a Lattice-Gas Model: Multiparticle Correlation Expansion*. Journal of Statistical Physics, 1999. **96**(1-2): p. 135-167.
10. S.D. Hong, *Evaluation of the excess free energy for two-center-Lennard-Jones liquids using the bent effective acceptance ratio*. Bulletin of the Korean Chemical Society, 2000. **21**(7): p. 697-700.
11. H. Do, J.D. Hirst, and R.J. Wheatley, *Rapid calculation of partition functions and free energies of fluids*. The Journal of Chemical Physics, 2011. **135**(17): p. 174105-7.
12. K.A. Fichthorn and W.H. Weinberg, *Theoretical Foundations of Dynamic Monte-Carlo Simulations*. Journal of Chemical Physics, 1991. **95**(2): p. 1090-1096.
13. C. Fan, D.D. Do, D. Nicholson, and E. Ustinov, *A novel application of kinetic Monte Carlo method in the description of N₂ vapour–liquid equilibria and adsorption*. Chemical Engineering Science, 2013. **90**(0): p. 161-169.
14. C. Fan, D.D. Do, and D. Nicholson, *New Monte Carlo simulation of adsorption of gases on surfaces and in pores: A concept of multibins*. The Journal of Physical Chemistry B, 2011. **115**(35): p. 10509-10517.
15. M. Abdul Razak, D.D. Do, T. Horikawa, K. Tsuji, and D. Nicholson, *On the description of isotherms of CH₄ and C₂H₄ adsorption on graphite from subcritical to supercritical conditions*. Adsorption, 2012: p. 1-12.
16. NIST, *Isothermal Properties for Argon*. 2011, NIST Chemistry WebBook.
17. R.B. Stewart and R.T. Jacobsen, *Thermodynamic Properties of Argon from the Triple Point to 1200 K with Pressures to 1000 MPa*. Journal of Physical and Chemical Reference Data, 1989. **18**(2): p. 639-798.
18. T.L. Hill, P.H. Emmett, and L.G. Joyner, *Calculation of Thermodynamic Functions of Adsorbed Molecules from Adsorption Isotherm Measurements: Nitrogen on Graphon_{1,2}*. Journal of the American Chemical Society, 1951. **73**(11): p. 5102-5107.
19. V.T. Nguyen, D.D. Do, and D. Nicholson, *Monte Carlo Simulation of the Gas-Phase Volumetric Adsorption System: Effects of Dosing Volume Size, Incremental Dosing Amount, Pore Shape and Size, and Temperature*. The Journal of Physical Chemistry B, 2011. **115**(24): p. 7862-7871.